

Contents lists available at [SciVerse ScienceDirect](http://www.sciencedirect.com)

Phytochemistry

journal homepage: www.elsevier.com/locate/phytochem

Characterization of two candidate flavone 8-*O*-methyltransferases suggests the existence of two potential routes to nevadensin in sweet basil

Anna Berim, David R. Gang*

Institute of Biological Chemistry, Washington State University, Pullman, WA 99164, USA

ARTICLE INFO

Article history:

Received 28 December 2012
 Received in revised form 7 March 2013
 Accepted 8 May 2013
 Available online xxxx

Keywords:

Ocimum basilicum L.
 Lamiaceae
 Sweet basil
 Biosynthetic network elucidation
 Lipophilic flavonoids
O-Methyltransferase
 Nevadensin
 Gardenin B

ABSTRACT

Regioselective 6-, 7-, 8-, 3'-, and 4'-*O*-methylations underlie the structural diversity of lipophilic flavones produced in the trichomes of sweet basil (*Ocimum basilicum* L.). The positions 6, 7, and 4' are methylated by a recently described set of cation-independent enzymes. The roles of cation-dependent *O*-methyltransferases still require elucidation. Here, the basil trichome EST database was used to identify a Mg²⁺-dependent *O*-methyltransferase that was likely to accept flavonoids as substrates. The recombinant protein was found to be active with a wide range of *o*-diphenols, and methylated the 8-OH moiety of the flavone backbone with higher catalytic efficiency than the 3'-OH group of candidate substrates. To further investigate flavone 8-*O*-methylation, the activity of a putative cation-independent flavonoid 8-*O*-methyltransferase from the same EST collection was assessed with available substrate analogs. Notably, it was strongly inhibited by gardenin B, one of its expected products. The catalytic capacities of the two studied proteins suggest that two alternative routes to nevadensin, a major flavone in some basil cultivars, might exist. Correlating the expression of the underlying genes with the accumulation of 8-substituted flavones in four basil lines did not clarify which is the major operating pathway *in vivo*, yet the combined data suggested that the biochemical properties of flavone 7-*O*-demethylase could play a key role in determining the reaction order.

© 2013 Elsevier Ltd. All rights reserved.

1. Introduction

Small molecule *O*-methyltransferases (OMTs) are subdivided into three classes (Noel et al., 2003). Class 1 and 2 OMTs are involved in methylation of mostly phenolic hydroxyl residues, whereas class 3 OMTs methylate carboxyl groups to yield methyl esters. The proteins are assigned to the different classes based on molecular size, cation requirement, and structure: class 1 comprises OMTs with a subunit molecular weight of 38–45 kDa and no cation dependency, while OMTs with smaller subunit size (22–27 kDa) and requiring a cation, usually magnesium, for activity belong to class 2. All of the above mentioned OMTs use *S*-adenosyl-L-methionine (SAM) as methyl group donor.

Early investigations of polymethoxylated flavonoid biosynthesis in golden saxifrage (*Chrysosplenium americanum*) and birdsfoot trefoil (*Lotus corniculatus*) suggested that some of the involved OMTs, e.g. the 6- and 8-OMT, required Mg²⁺ to be active (De Luca and

Ibrahim, 1982, 1985; Jay et al., 1985). However, plant Mg²⁺-dependent OMTs studied at the molecular level were thought to be specific for a single substrate, caffeoyl coenzyme A thioester (hence the designation CCoAOMTs or CCOMTs) and therefore to play pivotal roles in the biosynthesis of monolignols and related phenylpropanoids (Weng and Chapple, 2010), until a Mg²⁺-dependent OMT from ice plant (*Mesembryanthemum crystallinum*) was shown to catalyze the *O*-methylation of the flavonol quercetagenin at positions 6 and 3' (Ibdah et al., 2003). This CCoAOMT-like enzyme, as well as several putative homologs isolated in the same investigation, was also active with a number of phenylpropanoids and flavonoids, and formed a phylogenetically divergent OMT clade designated phenylpropanoid and flavonoid OMTs (PFOMTs) to reflect their multiple functions. Subsequently, other members of the PFOMT subclass were found to mediate the 3'-*O*- and in some cases also 5'-*O*-methylation of various subtypes of flavonoids, such as anthocyanins, flavonols, and flavones (Huguency et al., 2009; Lee et al., 2008; Lucker et al., 2010; Widiez et al., 2011). In addition, an OMT of this subclass contributes to the formation of spermidine-phenylpropanoid conjugates in *Arabidopsis* (Fellenberg et al., 2008). Some of the classical CCoAOMTs are capable of methylating flavonoids, albeit with lower efficiency than caffeoyl-CoA (Kim et al., 2010; Lukacin et al., 2004).

Abbreviations: SAM, *S*-adenosyl-L-methionine; (PF)OMT, (phenylpropanoid-flavonoid) *O*-methyltransferase.

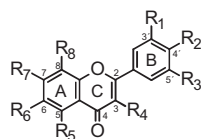
* Corresponding author. Tel.: +1 509 335 0550; fax: +1 509 335 7643.

E-mail address: gangd@wsu.edu (D.R. Gang).

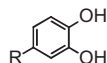
Sweet basil (*Ocimum basilicum* L.) accumulates lipophilic flavones with hydroxyl groups at positions 5, 6, 7, 8, 3', and 4' (Gray et al., 1996, 2001) (Table 1, compounds **1–7**, **13–16**) whose production appears to be confined to peltate trichomes (Berim et al., 2012). With the exception of the 5-OH, all hydroxyl residues are methylated in at least one of the accumulated flavones. While the recently investigated family of cation-independent OMTs was found to catalyze regioselective methylations at positions 6, 7, and 4' (Berim et al., 2012), the substrate- and regiospecificities of cation-dependent OMTs in basil have not yet been studied.

In this study, the basil trichome EST database (Gang et al., 2001) was used to identify representatives of class 2 OMTs in this cell type. Biochemical analysis of the most abundantly expressed candidate PFOMT indicated that it is a promiscuous enzyme whose *in vivo* role might depend on the availability of the accepted substrates and/or their subcellular localizations. As one of its potential functions is that of a flavonoid 8-O-methyltransferase (8-OMT), the activities of a candidate class 1 flavonoid 8-OMT were also evaluated. In addition, the correlation between the expression of the genes encoding these two proteins and the accumulation of the

Table 1
Structures of compounds used as substrates in this study and mentioned in the text, and relative activities of *Ob*PFOMT-1 and *Ob*F8OMT-1 with relevant compounds.



Name	R ₁	R ₂	R ₃	R ₄	R ₅	R ₆	R ₇	R ₈	Rel. activity (%) with	
									<i>Ob</i> PFOMT-1	<i>Ob</i> F8OMT-1
1 Gardenin B	H	OCH ₃	H	H	OH	OCH ₃	OCH ₃	OCH ₃		
2 Nevadensin	H	OCH ₃	H	H	OH	OCH ₃	OH	OCH ₃		
3 8-Hydroxy-salvigenin	H	OCH ₃	H	H	OH	OCH ₃	OCH ₃	OH		
4 Pilosin	H	OCH ₃	H	H	OH	OCH ₃	OH	OH		
5 Salvigenin	H	OCH ₃	H	H	OH	OCH ₃	OCH ₃	H		
6 Cirsimaritin	H	OH	H	H	OH	OCH ₃	OCH ₃	H		
7 Ladanein	H	OCH ₃	H	H	OH	OH	OCH ₃	H	10.5 ± 0.4	
8 Pectolinarigenin	H	OCH ₃	H	H	OH	OCH ₃	OH	H		
9 Scutellarein-7-methyl ether	H	OH	H	H	OH	OH	OCH ₃	H	11.4 ± 2.1	
10 Scutellarein-4'-methyl ether	H	OCH ₃	H	H	OH	OH	OH	H	122.5 ± 20	
11 Scutellarein	H	OH	H	H	OH	OH	OH	H	65.9 ± 0.5	
12 Scutellarin	H	OH	H	H	OH	OH	OGlcA	H	10.0 ± 1.3	
13 Eupatorin	OH	OCH ₃	H	H	OH	OCH ₃	OCH ₃	H		
14 Cirsilineol	OCH ₃	OH	H	H	OH	OCH ₃	OCH ₃	H		
15 Cirsiliol	OH	OH	H	H	OH	OCH ₃	OCH ₃	H	64.5 ± 0.4	
16 Genkwanin	H	OH	H	H	OH	H	OCH ₃	H		
17 Nepetin	OH	OH	H	H	OH	OCH ₃	OH	H	120.0 ± 3.4	
18 Diosmetin	OH	OCH ₃	H	H	OH	H	OH	H		
19 Chrysoeriol	OCH ₃	OH	H	H	OH	H	OH	H		
20 Luteolin	OH	OH	H	H	OH	H	OH	H	100.0 ± 4.5	
21 Luteolin-7-methyl ether	OH	OH	H	H	OH	H	OCH ₃	H	38.1 ± 0.3	
22 Luteolin-7-glucoside	OH	OH	H	H	OH	H	OGlc	H	57.3 ± 2.4	
23 Quercetagenin	OH	OH	H	OH	OH	OH	OH	H	13.8 ± 1.0	
24 Quercetin	OH	OH	H	OH	OH	H	OH	H	10.1 ± 0.4	
25 Quercetin-7-methyl ether	OH	OH	H	OH	OH	H	OCH ₃	H	11.2 ± 0.6	
26 Tricetin	OH	OH	OH	H	OH	H	OH	H	49.4 ± 1.1	
27 3',4'-OH-flavone	OH	OH	H	H	H	H	H	H	104.8 ± 2.8	
28 5,3',4'-OH-flavone	OH	OH	H	H	OH	H	H	H	64.3 ± 4.6	
29 7,3',4'-OH-flavone	OH	OH	H	H	H	H	OH	H	167.3 ± 4.4	
30 7,8,3',4'-OH-flavone	OH	OH	H	H	H	H	OH	OH	121.6 ± 0.9	12.6 ± 1.7
31 7,8,4'-OH-flavone	H	OH	H	H	H	H	OH	OH	222.2 ± 3.9	100.0 ± 1.4
32 7,8-OH-flavone	H	H	H	H	H	H	OH	OH	147.9 ± 7.3	32.1 ± 1.4
33 6,7-OH-flavone	H	H	H	H	H	OH	OH	H	54.2 ± 1.9	
34 5,6-OH-flavone	H	H	H	H	OH	OH	H	H	4.0 ± 1.0	
35 5,6-OH-7-OCH ₃ -flavone	H	H	H	H	OH	OH	OCH ₃	H	2.9 ± 0.3	
36 8-OH-7-OCH ₃ -flavone	H	H	H	H	H	H	OCH ₃	OH		62.2 ± 0.6
37 Eriodictyol (C ₂ -C ₃ bond saturated)	OH	OH	H	H	OH	H	OH	H	4.6 ± 0.2	



Name	R	Rel. activity (%) with	
		<i>Ob</i> PFOMT-1	<i>Ob</i> F8OMT-1
38 Caffeic acid	CH ₂ -CH=CH-COOH	78.0 ± 2.5	
39 3,4-OH-benzaldehyde	CHO	16.4 ± 0.2	
40 Catechol	H	3.3 ± 0.5	

Flavonoid ring nomenclature and carbon numbering are indicated on the generic backbone structure. OGlcA, O-glucuronide; OGlc, O-glucoside. The primary methyl acceptor residue is shown in bold. Turnover rates of *Ob*PFOMT-1 are presented relative to that with luteolin (100% = 1.54 nkat mg⁻¹ protein), all substrates were supplied at 50 μM. Turnover rates of *Ob*F8OMT-1 (B) are presented relative to that with 7,8,4'-OH-flavone (100% = 0.37 nkat mg⁻¹ protein), all substrates were supplied at 100 μM. Results are means ± S.E. (n = 3).

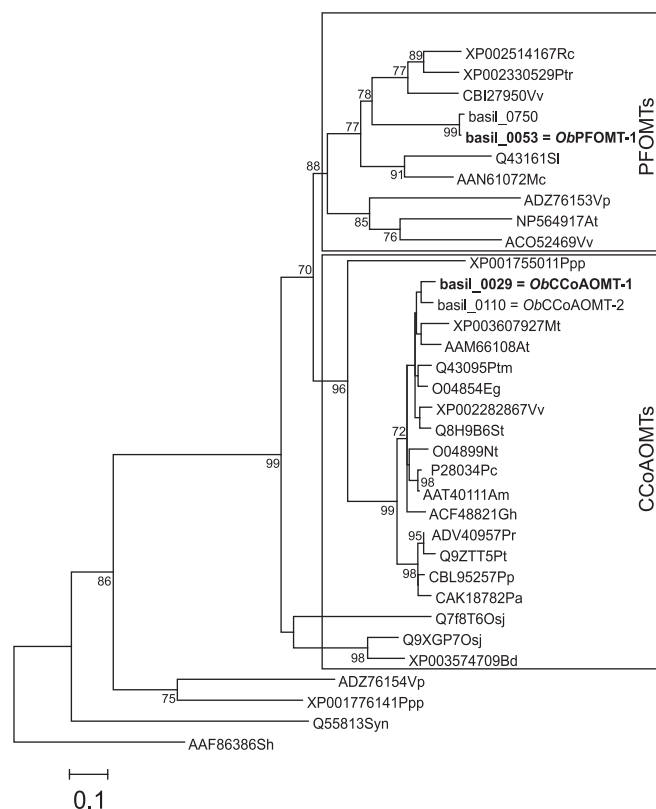


Fig. 1. Molecular phylogenetic analysis of selected cation-dependent OMTs by maximum likelihood method. Phylogeny was inferred using MEGA5 as described in Experimental, and tested by bootstrapping (500 replicates). Only bootstrap values greater than 70% are presented. Scale is in substitutions per amino acid. Basil proteins whose activities have been assessed are in bold. *FkbG* OMT from *Streptomyces hygroscopicus* (AAF86386Sh) was used as outgroup to root the tree. Branches are labeled with NCBI GenBank™ accession number and genus and species initials. Abbreviations are: Rc: *Ricinus communis*, Ptr: *Populus trichocarpa*, Vv: *Vitis vinifera*, Sl: *Stellaria longipes*, Mc: *Mesembryanthemum crystallinum*, Vp: *Vanilla planifolia*, At: *Arabidopsis thaliana*, Ppp: *Physcomitrella patens* subsp. *patens*, Mt: *Medicago truncatula*, Ptm: *Populus tremuloides*, Eg: *Eucalyptus gunnii*, St: *Solanum tuberosum*, Nt: *Nicotiana tabacum*, Pc: *Petroselinum crispum*, Am: *Ammi majus*, Gh: *Gossypium hirsutum*, Pr: *Pinus radiata*, Pt: *Pinus taeda*, Pp: *Pinus pinaster*, Pa: *Picea abies*, Osj: *Oryza sativa* cv. *japonica*, Bd: *Brachypodium distachion*, Syn: *Synechocystis* sp. (strain PCC 6803).

relevant 8-substituted flavones in young leaves of four basil lines was analyzed.

2. Results

2.1. Analysis of cation-dependent O-methyltransferases in the basil EST database

The basil trichome EST database (Gang et al., 2001) contains representatives of both CCoAOMT and PFOMT subclasses of the cation-dependent OMT family. Basil CCoAOMT contigs are abundantly represented, comprising more than 0.45% of total ESTs in the database. The encoded proteins share more than 90% identity with other known eudicot CCoAOMTs (Fig. 1). The protein designated *ObCCoAOMT-1*, encoded by a major contig basil_0029, was found to be active with coffeoyl-CoA (not shown). It is 91% identical to another full-length CCoAOMT contig (basil_0110, *ObCCoAOMT-2*) whose activities have not yet been assessed. Basil PFOMTs share ca. 60% identity with the basil CCoAOMTs, and are represented by eight contigs, two of them full-length, in the database. The encoded proteins form two groups differing essentially by four amino acids, equaling 98–100% identity on available

fragments (Supplemental Fig. S1). This high identity level strongly suggests functional redundancy. The most abundantly expressed contig (basil_0053) comprises 0.18% of the total ESTs, which amounts to about 10-fold of the abundance of ESTs in the other full-length PFOMT contig (basil_0750, Fig. 1). Basil PFOMTs are also ca. 60% identical to PFOMT from ice plant (Ibdah et al., 2003) and other known PFOMTs. Phylogenetic analysis confirmed that they belong to the PFOMT subfamily of the Mg^{2+} -dependent plant OMTs, and indicated that they cluster best with uncharacterized putative PFOMTs from castor bean (*Ricinus communis*) and grape (*Vitis vinifera*).

2.2. Biochemical characterization of *ObPFOMT-1*

This work focused on the protein encoded by the major contig basil_0053, which was provisionally designated *ObPFOMT-1*. The recombinant protein was produced in *E. coli* and purified using an N-terminal hexahistidine-tag (Supplemental Fig. S2). First analyses showed that *ObPFOMT-1* methylates the 3'-OH moiety of luteolin (20) and cirsiolol (15), two potential natural substrates (Fig. 2, traces 1, 2, Table 1). Its activity is highest in mildly alkaline solution at 30 °C (Supplemental Table S1). The optimal concentration of Mg^{2+} ions is different for different substrates (Supplemental Fig. S3). The cation concentration may therefore impact the reaction rates with competing flavones at the cellular level.

To find out what structural features are necessary for substrate recognition, *ObPFOMT-1* was incubated with luteolin derivatives lacking individual hydroxyl moieties, as well as a series of *ortho*-diphenols of varying structure. In summary, *ObPFOMT-1* appears to require vicinal hydroxyl groups and an electron-withdrawing moiety positioned *meta* to the methyl acceptor OH-group, as it was active with caffeic acid (38), 3,4-dihydroxybenzaldehyde (39), and 3',4'-OH-flavone (27), but only very low activity could be detected with eriodictyol (37), a flavanone derivative of luteolin (20) where the conjugation to the carbonyl moiety at C4 is interrupted, and with catechol (40), the simplest *ortho*-diphenol (Table 1, Supplemental Fig. S5). The majority of other characterized PFOMTs were found to display similarly broad substrate specificity (Fellenberg et al., 2008; Ibdah et al., 2003; Lee et al., 2008; Widiez et al., 2011).

2.2.1. Regioselectivity of *ObPFOMT-1*

Basil accumulates flavones whose backbones are additionally substituted at positions 6 and 8. *ObPFOMT-1* was therefore tested with a wide range of natural and unnatural flavones possessing two or three vicinal hydroxyl groups. These tests indicated that its regioselectivity varies with the structural context. In 5,6,7-trihydroxyflavones whose 7-OH moiety is methylated, such as scutellarein-7-methyl ether (9) and ladanein (7), the 5-OH moiety acts as the major methyl acceptor (Fig. 2 trace 3, Supplemental Fig. S4). Both of these substrates (7 and 9) belong to the flavone network in basil, yet their 5-O-methylated derivatives have not been reported to occur, suggesting that this activity of *ObPFOMT-1* has little or no relevance *in vivo*. In contrast, with unmethylated scutellarein (11) as substrate, it selectively catalyzes 6-O-methylation (Supplemental Fig. S4, trace 1). Scutellarin (12), the 7-O-glucuronide of scutellarein, is also predominantly methylated at position 6 despite the bulky vicinal sugar moiety (Supplemental Fig. S4, trace 2). The first methylation of quercetagenin (23) is also highly selective for the OH moiety at position 6 rather than 3' (Supplemental Fig. S4). Remarkably, incubation with tricetin (26), a flavone with 3',4',5'-hydroxylated ring B not accumulated by basil, results in three distinct products, one monomethylated and two dimethylated (Supplemental Fig. S4, trace 5). Because of this substrate's physiological irrelevance, unambiguous identification of these products was not pursued at this time point. However, a comparison with methylated tricetin derivatives used in the characterization of a class 1 OMT from wheat (Zhou

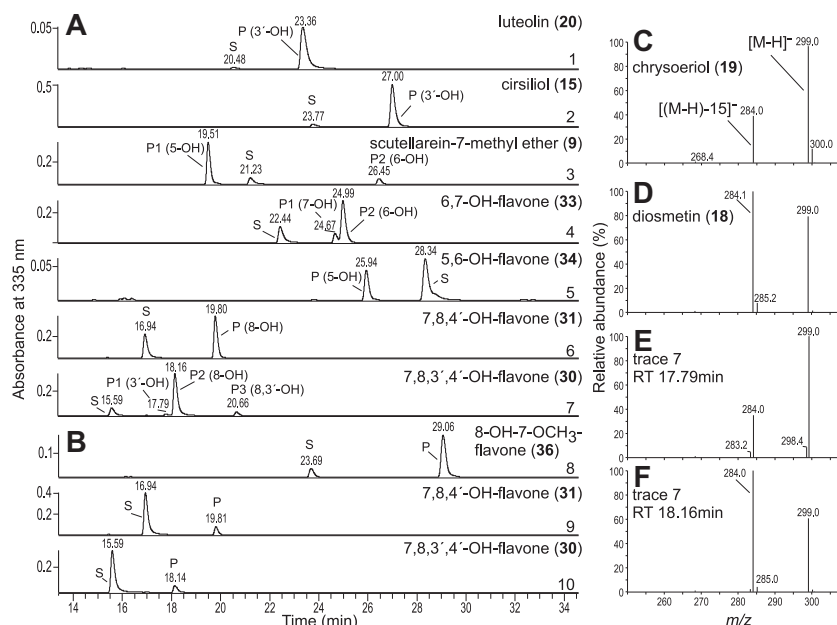


Fig. 2. Activities of *ObPFOMT-1* and *ObF8OMT-1* with selected substrates. **A** and **B**: Representative traces of reaction products of *ObPFOMT-1* (**A**, traces 1–7) and *ObF8OMT-1* (**B**, traces 8–10). Peaks labeled **S** are substrates, **P** are products. Methylation positions are indicated for *ObPFOMT-1*. Substrates are indicated on the right. Product of reaction in trace 1 was identified based on MS/MS spectrum comparison with authentic standards of chrysoeriol (**C**) and diosmetin (**D**). Based on fragmentation patterns (**E**, **F**) and comparisons with *ObF8OMT* (trace 10), product 1 (**P1**) in trace 7 tentatively identified as 3'-methyl ether (**E**), product 2 (**P2**) as 8-methyl ether (**F**) of 7,8,3',4'-OH-flavone. **C–F**. MS/MS fragmentation patterns used for product identification. Fragmentation of parent ions was achieved using negative ionization mode and 35% normalized collision energy as described in Section 5. Identity of fragment peaks is shown in **C** and is the same for **C–F**.

et al., 2006) indicates that the third acceptor moiety is the 4'-OH group (in addition to 3'- and 5'-OH). Additionally, a shift in the UV spectrum of the monomethylated product peak along the retention time and with progressing turnover suggests that it contains two products that are not chromatographically resolved and are methylated at 3'- or 4'-OH. This behavior is reminiscent of the Mg^{2+} -dependent OMT from the cyanobacterium *Synechocystis* (Q55813Syn, Fig. 1), which methylates both *meta* and *para* hydroxyl residues of di- and triphenols (Kopycki et al., 2008). Remarkably, it exhibited such relaxed regioselectivity only with cinnamic acid derivatives, while with tricetin as substrate it was specific for the 4'-OH group. In contrast, PFOMTs from vanilla (Widiez et al., 2011) and rice (Lee et al., 2008) were reported to be regiospecific for 3'- and 5'-OH groups of this substrate. *ObPFOMT-1* gives rise to two products with 6,7-OH-flavone (**33**), with 6-OH acting as the major acceptor group. Assays with 5,6-OH-flavone (**34**) and 7,8-OH-flavone (**32**) yielded 5-OH and 8-OH-methylated products, respectively (Fig. 2, Supplemental Fig. S4). Both 3'- and 8-OH-residues of 7,8,3',4'-OH-flavone (**30**) were methylated, however, the dominant acceptor appeared to be the hydroxyl residue at position 8, while the respective 3'-monomethyl ether was barely detectable (Fig. 2 trace 7). Therefore, at least for a substrate with this substitution pattern, 8-O-methylation is a more favorable reaction than the 3'-O-methylation.

Studies with the PFOMT from ice plant demonstrated that its N-terminus affected the protein's regioselectivity (Vogt, 2004). An analogously N-truncated (N-10) *ObPFOMT-1* variant was produced (Supplemental Fig. S2) and its activities tested with relevant substrates (**7**, **9**, **11**, and **30**), but no differences from the full-length protein were detected (not shown).

2.2.2. Relative activities with various substrates

Of the offered substrates, the highest relative reaction rates were measured with 7,8,4'-OH-flavone (**31**), 7,3',4'-OH-flavone (**29**), 7,8-OH-flavone (**32**), and scutellarein-4'-methyl ether (**10**) (Table 1, graphical overview in Supplemental Fig. S5). All of them can be excluded as natural substrates. Our previous work has established that

flavone 7-O-methylation is prerequisite for the subsequent 6-hydroxylation (Berim and Gang, 2013), therefore, scutellarein-4'-methyl ether does not serve as an intermediate and is unlikely to be present in basil in appreciable amounts at any time. The former three compounds are unnatural, synthetic flavones. However, the 7,8-dihydroxyl substitution pattern of the ring A in substrates **31** and **32** is reminiscent of pilosin (**4**), which accumulates in some basil varieties (Grayer et al., 2001, Section 2.4 of this work), but is not currently available to us. The relative activities with basil flavones scutellarein-7-methyl ether (**9**) and ladanein (**7**) were under 25% of that found with luteolin (**20**). Cirsiolol (**15**) was considered an auspicious substrate as its 3'-O-methylated derivative cirsiolol (**14**) occurs in basil (Grayer et al., 1996). However, the relative turnover with **15** only amounted to 64% of that with luteolin (**20**). Notably, it was observed that higher cation concentrations (100 μM vs. 10 μM Mg^{2+}) reduce the relative turnover rates of 7-O-methylated substrates **7** and **9** by ca. 12% and 30%, respectively, but significantly increase that of caffeic acid (**37**) (27% vs. 78%). As this effect might extend to other substrates, the results shown in Table 1 and Supplemental Fig. S5 should be viewed as specific for the assay conditions used. The cytosolic concentrations of free Mg^{2+} vary between different cell types and subcellular compartments, usually not exceeding 2 mM in cytosol (Bose et al., 2011) where the OMT reactions are likely to occur, and have never been estimated for secretory cells of peltate trichomes. It is therefore impossible to predict how this will influence the reaction rates *in vivo*.

2.2.3. Kinetic properties

Kinetic analyses showed that 7,8,4'-OH-flavone (**31**), which is methylated at position 8 by *ObPFOMT-1*, is converted with higher catalytic efficiency and is therefore a better substrate than luteolin (**20**) and cirsiolol (**15**) (Table 2). The apparent affinity constants in low micromolar range are typical and physiological for many of the reported O-methyltransferases (Fellenberg et al., 2008; Ibdah et al., 2003; Lucker et al., 2010). However, all of the enzymes involved in flavone biosynthesis in basil that have been studied to date displayed much higher affinity for their proposed physiological

Table 2
Kinetic properties of *ObPFOMT-1* and *ObF8OMT-1* with selected substrates.

Enzyme	Substrate	K_m (μM)	V_{max} (nkat mg^{-1})	k_{cat} (s^{-1}) $\times 10^{-3}$	k_{cat}/K_m ($\text{s}^{-1}\text{mM}^{-1}$)
<i>ObPFOMT-1</i>	Luteolin (20) ^a	3.98 \pm 0.36	1.61 \pm 0.03	45.39 \pm 0.93	11.38
	Cirsiliol (15) ^a	8.62 \pm 0.50	1.22 \pm 0.06	34.30 \pm 1.63	3.98
	7,8,4'-OH-flavone (31) ^a	3.31 \pm 0.42	4.30 \pm 0.21	121.1 \pm 5.87	36.61
	SAM ^b	12.19 \pm 1.42	1.94 \pm 0.08	54.77 \pm 2.28	4.49
<i>ObF8OMT-1</i>	7,8,4'-OH-flavone (31) ^{a,c}	4.69 \pm 0.12	0.39 \pm 0.07	16.71 \pm 3.04	3.57
	7-OCH ₃ -8-OH-flavone (36) ^{a,c}	7.82 \pm 0.50	0.25 \pm 0.01	10.75 \pm 0.29	1.38
	7,8-OH-flavone (32) ^{a,c}	6.99 \pm 0.39	0.11 \pm 0.01	4.61 \pm 0.37	0.66
	SAM ^d	1.78 \pm 0.22	0.41 \pm 0.05	17.79 \pm 0.22	9.49

^a Reactions were performed with 50 μM SAM as cosubstrate.

^b Reactions were performed with 50 μM luteolin as substrate.

^c Results are means \pm S.E. ($n = 4$), for all other series results are means \pm S.E. ($n = 3$).

^d Reactions were performed with 100 μM 7,8,4'-OH-flavone as substrate.

substrates, as reflected by ca. 10- to 100-fold lower apparent K_m values (Berim and Gang, 2013; Berim et al., 2012). As stated above, the only naturally occurring basil flavone that could act as a substrate for 8-*O*-methylation by *ObPFOMT-1*, pilosin (**4**), is presently not available from any source. Considering the fact that no uncharacterized ESTs in our current database seem to correspond to the flavonoid 3'-OMT from peppermint (Willits et al., 2004), *ObPFOMT-1* remains the most promising candidate to fulfill this function in basil. An analysis of other steps involved in the accumulation of 3'-substituted flavones (e.g. the activities of flavone 6- and 3'-hydroxylases with relevant substrates) is necessary to delineate this side branch of flavone network in basil trichomes.

2.3. Properties of the cation-independent putative flavonoid 8-OMT from basil

The above data indicate that *ObPFOMT-1* could be involved in methylation of pilosin (**4**) to yield nevadensin (**2**). However, based on our prior results (Berim and Gang, 2013; Berim et al., 2012), gardenin B (**1**) originates from the methylation of 8-hydroxysalvigenin (**3**), whereas the 7-*O*-methylation of nevadensin (**2**) is a very slow and probably negligible process. As *ObPFOMT-1* does not catalyze the methylation of 8-OH-7-OCH₃-flavone (**36**) and in general requires vicinal hydroxyl residues for activity, it is not expected to be involved in this step.

Prior to the analysis of the cation-dependent OMTs it seemed likely that the 8-*O*-methylation is carried out by a class 1 OMT, a homolog of F8OMT from peppermint (Willits et al., 2004). The basil EST database contains four contigs sharing ca. 67% identity with that enzyme. This identity level is similar to those found for flavone 7- and 4'-OMTs in the two species (Berim et al., 2012). The four contigs are >90% identical, yet the activities of the encoded proteins may differ. The most abundantly expressed putative 8-OMT (termed *ObF8OMT-1*) was chosen for heterologous expression and preliminary biochemical characterization (for some basic properties, see Supplemental Table S1). *ObF8OMT-1* was active with all four available 8-substituted flavones (Fig. 2, Table 1), and displayed the most favorable kinetics with 7,8,4-hydroxyflavone (**31**) (Table 2). The relative reaction rates with the offered substrates differed from those determined for the peppermint F8OMT, which showed highest turnover with 8-OH-7-OCH₃-flavone (**36**) (Willits et al., 2004). As found for *ObPFOMT-1*, the apparent affinity constants were in the low micromolar range, yet far higher than those determined for other enzymes involved in flavone metabolism in basil (Berim and Gang, 2013; Berim et al., 2012). Kinetic properties suggest that the presence of a 7-*O*-methyl moiety improves the catalytic efficiency, possibly indicating that 8-hydroxysalvigenin (**3**) would be a better substrate than pilosin (**4**) (Table 2). However, only experimental data with **3** and **4** will allow us to make definitive conclusions regarding the preferred natural substrate of *ObF8OMT-1*. Importantly, *ObF8OMT-1* is strongly inhibited by gardenin B (**1**),

the product of 8-hydroxysalvigenin 8-*O*-methylation (Fig. 3). Plotting the data according to Dixon (1953) indicated competitive inhibition as the underlying mechanism and a very low K_i value of ca. 10–15 nM (Fig. 3B). Nevadensin (**2**), the product of pilosin (**4**) 8-*O*-methylation, which differs from gardenin B (**1**) by one methyl group at position 7, does not exert a measurable inhibitory effect, nor does genkwaniin (**16**), a 7-*O*-methylated flavone occurring in basil. None of these flavones inhibit *ObPFOMT-1* (Fig. 3A). Overall, this suggests that the inhibition of *ObF8OMT-1* by gardenin B is highly specific. Whether it becomes physiologically important depends on the concentration of gardenin B in the catalytically active compartment, the secretory cells of the trichomes, as well as on the affinity of *ObF8OMT-1* for its natural substrate(s) and their abundance. Our previous results implied that lipophilic flavones including gardenin B

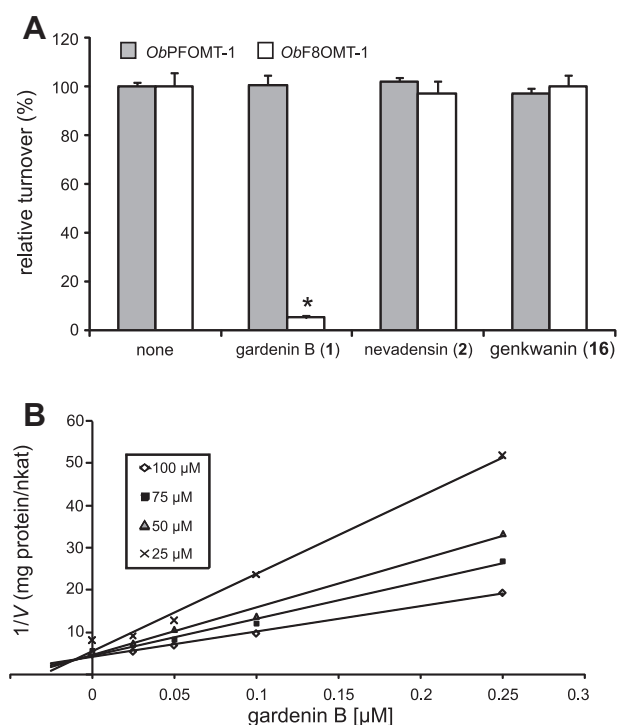


Fig. 3. Inhibition of *ObPFOMT-1* and *ObF8OMT-1* by selected basil flavones. A. Turnover measured in reactions supplied with 2.5 μM of tested inhibitor. Turnover of *ObPFOMT-1* with luteolin (50 μM) and of *ObF8OMT-1* with 8-OH-7-OCH₃-flavone (100 μM) without inhibitor addition was set as 100%. Results are means \pm S.D. ($n = 3$). Asterisk indicates data point statistically different from control according to Student's *t*-test ($P = 0.0007$). All other means were not statistically different from control ($P > 0.05$). B. Dixon plot of *ObF8OMT-1* inhibition by gardenin B. Concentrations of 8-OH-7-OCH₃-flavone (substrate) are indicated in the legend. Intercept served for the estimation of a K_i value of ca. 10 nM. Assays were performed in triplicates, means are shown.

(1) are enriched in the subcuticular cavities of mature trichomes (Berim et al., 2012), but there are presently no data regarding the time course of their translocation or the reversibility of this process.

2.4. Expression of *ObPFOMT-1* and *ObF8OMT-1* and accumulation of relevant flavones in four basil cultivars

The EST counts for *ObPFOMT-1* and *ObF8OMT-1* suggest that these genes are expressed at different levels in the four basil lines routinely used in our lab, for example, no ESTs coding for *ObF8OMT-1* originate from the line MC. In order to verify this, the transcript levels were assessed using qRT-PCR. In a preliminary experiment, the mRNA levels in isolated trichomes were estimated. The trends were in agreement with the EST counts, confirming high expression of *ObPFOMT-1* in all lines and significantly higher expression of *ObF8OMT-1* in the lines EMX-1 and SD as compared to the lines SW and MC (Fig. 4). The expression of *ObPFOMT-1* and *ObF8OMT-1* was then correlated with the accumulation of relevant flavones in the youngest leaf pair on a stem with seven leaf pairs. The expression profiles in whole leaves were very similar to those found in isolated trichomes (Fig. 4). The *ObPFOMT-1* transcripts were most abundant in the line EMX-1, whereas *ObF8OMT-1* was barely detectable in the lines MC and SW. For the metabolite analysis, liquid chromatography conditions were modified to separate the isobaric flavones neavadensin (2) and 8-hydroxysalvigenin (3), which were previously quantified as one compound. Flavone profiles were similar in lines SD and EMX-1 and differed from those in the lines SW and MC (Fig. 5). Whereas in the former two lines neavadensin is the major flavone with m/z 345, in the latter cultivars it is 8-hydroxysalvigenin. Neavadensin is a minor metabolite in these lines (SW and MC). Pilosin (4) accumulates in amounts comparable to those of gardenin B (1) in line SD, but not in the other

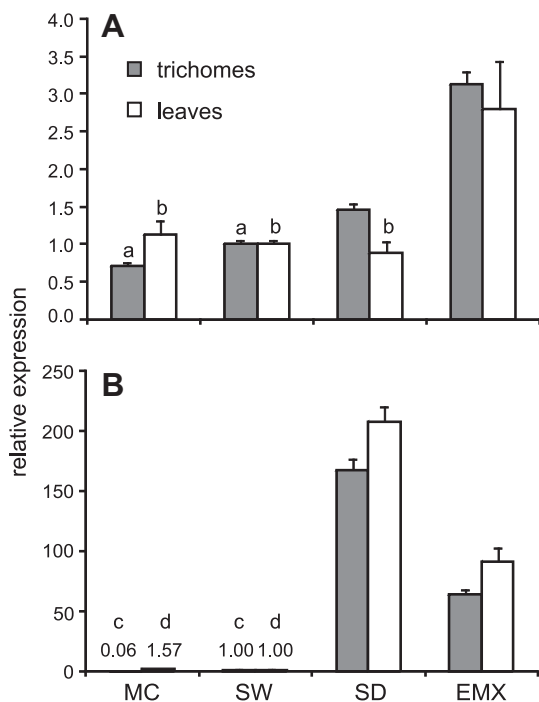


Fig. 4. Expression of *ObPFOMT-1* (A) and *ObF8OMT-1* (B) in whole leaves and isolated trichomes of four basil lines. Transcript levels of *ObPFOMT-1* and *ObF8OMT-1* in the 7th leaf pair and in isolated trichomes of four basil lines were assessed using qRT-PCR. Legend indicates which tissue was used. Expression in the line SW was set as 1 for both genes and each tissue. Results are means \pm S.E. of five biological replicates for whole leaves, and means \pm S.E. of three technical replicates for isolated trichomes. Values are indicated on the graph where not easily legible. Means of data points marked with the same letter are not statistically different according to one-way ANOVA and Tukey's HSD post hoc tests ($P < 0.05$).

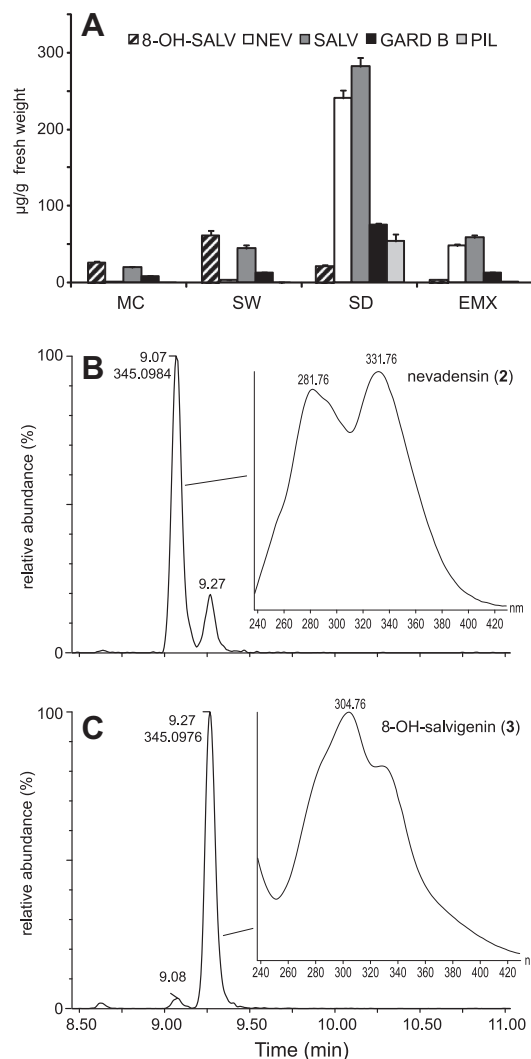


Fig. 5. Accumulation of selected flavones in young leaves of four basil lines. A. Amounts of 8-hydroxysalvigenin (3) (8-OH-SALV), neavadensin (2) (NEV), salvigenin (5) (SALV), gardenin B (1) (GARD B), and pilosin (4) (PIL) in the 7th leaf pair of four basil lines. Results are means \pm s.e. of 5 biological replicates. B. and C. Representative chromatograms (shown at m/z 345.0969 \pm 10 ppm) of UPLC separation of isobaric flavones 8-OH-salvigenin (3) and neavadensin (2) as described in Section 5 and an extract from the line EMX-1 (B) and SW (C) as analyte. Insets show respective UV-spectra.

three lines. Because of the large differences in absolute accumulation of flavones in the different basil lines, it is important to consider the relative proportions of the individual flavones, setting the total amount of monitored compounds as 100%. The proportion of salvigenin (5) is 34–46% in all lines. The relative abundances of gardenin B range between 10–14% in all four lines. Neavadensin takes up 35–40% of the total in lines SD and EMX-1, whereas 8-hydroxysalvigenin accounts for about 50% of monitored flavones in the lines SW and MC.

As *ObPFOMT-1* may act as flavone 3'-OMT, the abundance of potential product, cirsilineol (14) was also monitored in the different basil lines. As it proved difficult to separate it from its isomer, eupatorin (15) (Grayer et al., 1996, 2001; our work), both were co-quantified. Their amounts were below reliable quantification level in line MC, while lines EMX-1, SD, and SW accumulated 5.71, 15.66, and 10.47 μ g per g fresh weight, respectively. Because of their very different ionization efficiencies in negative ionization mode in our LCQ Advantage mass spectrometer, it is permissible to estimate that cirsilineol (14) accounts for nearly 100% of the

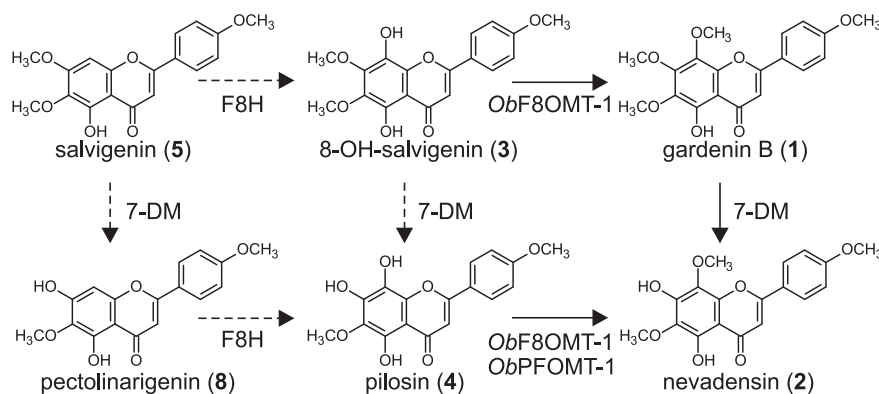


Fig. 6. Potential steps around flavone 8-*O*-methylation in sweet basil. Solid arrows indicate conversions supported by evidence (including this work), dashed arrows indicate there is no current data as to whether or how such a step occurs. F8H, flavone 8-hydroxylase; 7-DM, flavone 7-*O*-demethylase.

detected joint amount in the line EMX-1, about 50% in the line SD, and 5% in the line SW.

3. Discussion

Our recent investigation indicated that 7-*O*-methylation is a prerequisite for flavone 6-hydroxylation, and that the occurrence of 7-unmethylated flavones nevadensin (**2**) and pilosin (**4**) is due to oxoglutarate-dependent 7-*O*-demethylation in basil trichomes (Berim and Gang, 2013). Integration of the biochemical findings presented above into the emerging scheme of this biosynthetic network implies that there are two potential routes yielding nevadensin (**2**), one of the major flavones in basil cultivars SD and EMX-1 (Fig. 6). One of them proceeds via gardenin B (**1**), and involves its 7-*O*-demethylation as the last step. Demethylation of gardenin B (**1**) has been demonstrated in crude trichome protein extracts (Berim and Gang, 2013). The other route positions pilosin (**4**) as the immediate precursor of nevadensin. *ObF8OMT-1* would be involved in both cases, while *ObPFOMT-1* only plays a role in the accumulation of nevadensin if the second scenario is the major one. Based on metabolic analysis indicating that pectolarigenin (**8**) does not accumulate in basil leaves (Berim et al., 2012) and on preliminary data that 7-*O*-demethylation of salvigenin (**5**) does not readily occur in trichome protein extracts under the conditions used to detect the demethylation of gardenin B (**1**) (Berim and Gang, unpublished), the formation of pilosin (**4**) itself is predicted to occur via the 7-*O*-demethylation of 8-hydroxysalvigenin (**3**). So far, the lack of the proposed substrate prevents us from investigating this hypothesis further.

Analysis of relevant metabolites and transcript levels of both candidate 8-OMTs in the four basil lines does not resolve this ambiguity. The high proportion of 8-hydroxysalvigenin (**3**) relative to gardenin B (**1**), pilosin (**4**) and nevadensin (**2**) in the cultivars SW and MC is in line with the notion that only a small portion of it is converted further, matching well with the low expression of *ObF8OMT-1*, and suggesting that 7-*O*-demethylation is a minor process in these two lines. The fact that lines SW and MC accumulate gardenin B (**1**) despite the low expression of *ObF8OMT-1* can indicate that even this low expression level suffices to support measurable conversion. It can also be in part due to the presence of divergent minor contigs not amplified by the used qPCR primers. Overall, the seemingly absent 7-*O*-demethylase activity and therefore non-occurrence of the proposed substrate pilosin (**4**) make it impossible to draw conclusions regarding the actual reaction order and the role of *ObPFOMT-1* in 8-*O*-methylation from these two basil lines. In the cultivars SD and EMX-1, the relative abundance of 8-hydroxysalvigenin (**3**) is low. *ObF8OMT-1* is well expressed in these two basil lines; however, the

relative abundances of gardenin B (**1**) are comparable to those found in the lines MC and SW. On the one hand, this could be due to further conversion of gardenin B into nevadensin (**2**). On the other hand, this flavone profile could result from the strong inhibition of *ObF8OMT-1* by gardenin B (**1**), coupled with highly active 7-*O*-demethylation of 8-hydroxysalvigenin (**3**) to yield pilosin (**4**). In line EMX-1, pilosin (**4**) itself would be further converted into nevadensin (**2**) by the more abundantly expressed *ObPFOMT-1*, whereas in line SD it would be in part stored. Optionally, the accumulation of pilosin (**4**) in line SD may depend on a distinct 8-hydroxysalvigenin-specific 7-*O*-demethylase whose expression is low in line EMX-1. In absence of other data, all of the above interpretations appear equally legitimate.

Despite the limitations posed by the lack of natural substrates, this work provides further valuable insights into a presently only poorly understood segment of flavone metabolism in basil by identifying an unanticipated candidate 8-OMT and highlighting the ambiguity regarding the major direct precursor of nevadensin. Currently, direct genetic means (e.g. transgenic techniques) that could provide final clarity for the primary operating pathway as well as for the respective contributions of these two OMTs to the observed flavone profiles in basil are still under development. Obviously, a better characterization of *ObPFOMT-1* and *ObF8OMT-1* with the proposed natural 8-OMT substrates (**3** and **4**) would be indispensable to estimate the efficiency and thus the likelihood of their involvement in the respective conversions. As *ObPFOMT-1* displays relaxed substrate specificity with simple *o*-diphenols, its high 8-*O*-methylating activity might be an *in vitro* artifact. Indeed, two cation-dependent OMTs from rice were also active with 7,8-OH-flavone (**32**), and position 8 was suggested to be the methylation site (Lee et al., 2008). It can also be expected that the characterization of 7-*O*-demethylase(s) will shed more light on the actual routes and processes underlying the formation of nevadensin in basil. We will use the presumed low expression of the underlying dioxygenase(s) in SW and MC as compared to SD and EMX-1 as a criterion to help narrow down our choices of candidate genes. Alternatively, identification of a basil cultivar/variety displaying low expression of the *ObPFOMT-1* gene but high 7-*O*-demethylase and *ObF8OMT-1* activity might offer insights into the respective gene's functions in the plant.

4. Concluding remarks

The above work presents another step towards the complete biochemical elucidation of the flavone metabolic network in basil. This study suggests that the roles of cation-dependent OMTs in basil might not be limited to 3'-*O*-methylation, and draws our attention to the conundrum surrounding the two potential routes to

nevadensin (**2**). Our next objective is to procure the currently unavailable substrates, pilosin (**4**) and 8-hydroxysalvigenin (**3**), which should be used to study the activities and kinetic properties of the described methyltransferases, as well as the 7-*O*-demethylase(s). The elucidation of the latter step, the oxoglutarate-dependent demethylation of 8-hydroxysalvigenin (**3**) and/or gardenin B (**1**), may be of critical importance for an accurate assessment of the true reaction order leading to the distinct profiles of 8-substituted flavones in basil.

5. Experimental

5.1. General

Unless noted otherwise, chemicals were of analytical quality and purchased from common vendors (Fisher Scientific, VWR International, Sigma Aldrich). Molecular biology reagents were from Invitrogen and New England Biolabs. Rosetta™ 2 (DE3)pLysS cells (Novagen) were used for heterologous gene expression. S-adenosyl-[¹⁴C-methyl]-L-methionine (48.8 mCi/mmol) was obtained from Perkin Elmer. Unlabeled SAM, caffeic acid (**38**), 3,4-OH-benzaldehyde (**39**), and catechol (**40**), were from Sigma Aldrich. All synthetic flavones were purchased from Indofine. Quercetagenin (**23**) and tricetin (**26**) were from Extrasynthese. The sources of all other naturally occurring flavonoids and authentic basil flavones were the same as previously described (Berim et al., 2012). Authentic samples of gardenin B (**1**), nevadensin (**2**), and eupatorin (**13**) were kindly donated by Dr. R. Grayer (Kew RBG, London, UK).

5.2. Plant material growth and culture

Basil seeds (*O. basilicum* lines EMX-1, SW, MC, and Sweet Dani [SD]) were germinated in vermiculite and individually re-potted into SunGro mix. Plants were grown in growth chambers under 16/8 photoperiod and 28 °C (24 h). Light intensity of ca. 300 μmol m⁻² s⁻¹ was supplied by incandescent and fluorescent lamps.

5.3. Metabolite extracts

Flavones were extracted using the protocol reported earlier (Berim et al., 2012). Whole small leaves (1–1.5 cm length, 7th leaf pair from a stem with seven leaf pairs) were used for extraction. Five biological replicates were collected for each basil line.

5.4. Metabolite and enzyme assay analyses

The same instrumentation (ion trap system: LCQ Advantage system with Surveyor HPLC and photodiode array detector (Thermo), and Q-TOF-MS system: Synapt G2 quadrupole-ion mobility spectrometry-time of flight mass spectrometer system (Waters) equipped with an Acquity UPLC system with photodiode array detector) as described previously (Berim et al., 2012) was used for metabolite and enzyme assay product analysis. The MS settings for positive mode electrospray ionization and the Q-TOF-MS source conditions were also as reported previously. Negative mode ionization (using the above mentioned LCQ Advantage system) was applied to distinguish between chrysoeriol (**19**) and diosmetin (**18**), as well as eupatorin (**13**) and cirsiolineol (**14**). In this case, tuning was carried out with apigenin. The optimized MS settings were as follows: capillary at 275 °C and –21 V, source at 5.0 kV and spray current at 30 μA, sheath/sweep gas flow at 33/20 (arbitrary units). For collision-induced dissociation spectra, fragmentation was achieved using 35% normalized collision energy and

data-dependent mode. Separation of nevadensin (**2**) and 8-hydroxysalvigenin (**3**) using a previously described UPLC system (Berim et al., 2012) was achieved using an Acquity HSS T3 UPLC® column (100 × 2.1 mm, 1.7 μm, Waters). The linear gradient used the same solvents as other separations, with a flow rate of 400 μL min⁻¹, and ran as follows: 0 min, 5% B; 0.86 min, 5% B; 6.00 min, 40% B; 12.00 min, 48% B; 14.00 min, 100% B; 16.00 min, 100% B; 17.00 min, 5% B; 20.00 min, 5% B. Quantification was based on standard curves produced using serial dilutions of authentic compounds eupatorin (**13**), nevadensin (**2**) and gardenin B (**1**). Under the previously made assumption of ca. equal UV₃₃₅ extinction coefficients (Grayer et al., 1996), the standard curve for nevadensin was used to estimate the amounts of 8-hydroxysalvigenin (**3**) and pilosin (**4**).

5.5. RNA extraction

RNA for cloning purposes and for quantification of *ObPFOMT-1* and *ObF8OMT-1* transcripts was isolated and its quality checked as described previously (Berim et al., 2012).

5.6. Cloning and heterologous expression of basil OMTs

Primers shown in Supplemental Table S2 were used to obtain the full length clones which were subcloned into pCR2.1® TOPO® vector (Invitrogen) followed by transfer to pET15b (Novagen) for expression. Heterologous expression and protein purification were conducted as reported earlier (Berim et al., 2012).

5.7. Biochemical characterization

For quantitative analyses, reaction conditions were chosen so that the reaction velocity was directly proportional to incubation time and protein amount. For kinetics measurements, saturating concentrations of the second substrate (flavone or SAM) were provided. Affinities for SAM were determined using luteolin (*ObPFOMT-1*) or 7,8,4'-OH-flavone (*ObF8OMT-1*) as substrate.

Energy of activation and thermal stability were determined using 50 mM K-Pi pH 8.5 (*ObPFOMT-1*) or 7.5 (*ObF8OMT-1*) buffer and 10 mM MgCl₂ (*ObPFOMT-1*). Dependency of reaction rates on pH was determined using the same buffer systems as reported earlier (Berim et al., 2012).

Radioactive assays were carried out in a total volume of 100 μL, incubated at 30 °C for an appropriate length of time (including 5 min pre-conditioning), quenched with 5 μL 6 N HCl, and extracted with 200 μL EtOAc. A standard assay for *ObPFOMT-1* contained 100 mM Tris/HCl pH 8.5, 10 μM MgCl₂, 50 μM substrate (luteolin), 0.4 μg purified protein, and was started with 50 μM SAM. Assay series for substrate comparison with *ObPFOMT-1* were supplied with 100 μM MgCl₂. A standard assay for *ObF8OMT-1* contained 100 mM Tris/HCl pH 7.5, 100 μM substrate (7,8,4'-OH-flavone), 0.6 μg purified protein, and was started as above. After centrifugation for 3 min at 21,000g, an aliquot of the upper phase was added to Eco-Scint scintillation cocktail (5 mL) (National Diagnostics) and analyzed using RackBeta 1215 scintillation counter (LKB). Relative reaction rates with a range of flavones were measured with 50 μM (*ObPFOMT-1*) or 100 μM (*ObF8OMT*) substrate and 50 μM SAM. Assays with unlabeled SAM (supplied at 200 μM) for product identification were carried out in a total volume of 100 μL under appropriate conditions, stopped with 6 N HCl (10 μL) and the aq. phase extracted with EtOAc (2 × 200 μL). After evaporating the combined organic phases, the dry residue was dissolved in MeOH-LC buffer (5 mM ammonium formate/0.1% HCO₂H) ((50 μL) 1:1, v/v) and analyzed using the LCQ as described above and earlier (Berim et al., 2012).

5.8. Phylogenetic analysis of sweet basil OMTs

Selected (putative) PFOMT protein sequences were retrieved from NCBI GenBank™ and from basil EST database. Duplicates (contigs encoding identical peptides) and peptides shorter than 1/3 of the expected OMT length were removed. Resulting sequences were aligned using Clustal W2 at EBI with default settings. MEGA5 package (Tamura et al., 2011) was used for the phylogenetic analysis and tree construction. Evolutionary relationships were inferred using maximum likelihood algorithm and Jones-Taylor-Thornton matrix. All sites, independently of coverage, were used for analysis. The tree was rooted using *fkbg* OMT from *Streptomyces hygroscopicus* (AAF86386Sh) as outgroup.

5.9. Quantitative real-time RT-PCR

The relative quantification method (Schmittgen and Livak, 2008) was used to assess the abundances of transcripts. Protocol optimization, general considerations and instrumentation were as reported previously (Berim et al., 2012). Primers are listed in Supplemental Table S2. *Elongation factor 1* gene served as reference for normalization. For scaling, the relative expression of both genes in the line SW was set as 1 for each tissue. Five biological replicates of each leaf pair, and three technical replicates of one trichome preparation of each basil line were analyzed.

6. Accession numbers

Coding sequences for *ObPFOMT-1* and *ObF8OMT-1* were submitted to NCBI GenBank™ under accession numbers KC354401 and KC354402, respectively.

Acknowledgements

We thank Dr. R. Grayer (Kew RBG, London, UK) for the authentic samples of nevadensin, eupatorin, and gardenin B. This work was supported by the DOE Biological and Environmental Research Program Grant DE-SC0001728 to D.R.G.

Appendix A. Supplementary data

Supplementary data associated with this article can be found, in the online version, at <http://dx.doi.org/10.1016/j.phytochem.2013.05.001>.

References

- Berim, A., Gang, D.R., 2013. The roles of a flavone 6-hydroxylase and 7-O-demethylation in the flavone biosynthetic network of sweet basil. *J. Biol. Chem.* 288, 1795–1805.
- Berim, A., Hyatt, D.C., Gang, D.R., 2012. A set of regioselective O-methyltransferases gives rise to the complex pattern of methoxylated flavones in sweet basil. *Plant Physiol.* 160, 1052–1069.
- Bose, J., Babourina, O., Rengel, Z., 2011. Role of magnesium in alleviation of aluminium toxicity in plants. *J. Exp. Bot.* 62, 2251–2264.
- De Luca, V., Ibrahim, R.K., 1982. Characterization of three distinct flavonol O-methyltransferases from *Chrysosplenium americanum*. *Phytochemistry* 21, 1537–1540.
- De Luca, V., Ibrahim, R.K., 1985. Enzymatic synthesis of polymethylated flavonols in *Chrysosplenium americanum*. I. Partial purification and some properties of S-adenosyl-L-methionine:flavonol 3, 6, 7, and 4'-O-methyltransferases. *Arch. Biochem. Biophys.* 238, 596–605.
- Dixon, M., 1953. The determination of enzyme inhibitor constants. *Biochem. J.* 55, 170–171.
- Fellenberg, C., Milkowski, C., Hause, B., Lange, P.-R., Boettcher, C., Schmidt, J., Vogt, T., 2008. Tapetum-specific location of a cation-dependent O-methyltransferase in *Arabidopsis thaliana*. *Plant J.* 56, 132–145.
- Gang, D.R., Wang, J.H., Dudareva, N., Nam, K.H., Simon, J.E., Lewinsohn, E., Pichersky, E., 2001. An investigation of the storage and biosynthesis of phenylpropanes in sweet basil. *Plant Physiol.* 125, 539–555.
- Grayer, R.J., Bryan, S.E., Veitch, N.C., Goldstone, F.J., Paton, A., Wollenweber, E., 1996. External flavones in sweet basil, *Ocimum basilicum*, and related taxa. *Phytochemistry* 43, 1041–1047.
- Grayer, R.J., Veitch, N.C., Kite, G.C., Price, A.M., Kokubun, T., 2001. Distribution of 8-oxygenated leaf-surface flavones in the genus *Ocimum*. *Phytochemistry* 56, 559–567.
- Huguency, P., Provenzano, S., Verries, C., Ferrandino, A., Meudec, E., Batelli, G., Merdinoglu, D., Cheynier, V., Schubert, A., Ageorges, A., 2009. A novel cation-dependent O-methyltransferase involved in anthocyanin methylation in grapevine. *Plant Physiol.* 150, 2057–2070.
- Ibdah, M., Zhang, X.H., Schmidt, J., Vogt, T., 2003. A novel Mg(2+)-dependent O-methyltransferase in the phenylpropanoid metabolism of *Mesembryanthemum crystallinum*. *J. Biol. Chem.* 278, 43961–43972.
- Jay, M., DeLuca, V., Ibrahim, R.K., 1985. Purification, properties and kinetic mechanism of flavonol 8-O-methyltransferase from *Lotus corniculatus* L. *Eur. J. Biochem.* 153, 321–325.
- Kim, B.-G., Kim, D.H., Sung, S.H., Kim, D.-E., Chong, Y., Ahn, J.-H., 2010. Two O-methyltransferases from *Picea abies*: characterization and molecular basis of different reactivity. *Planta* 232, 837–844.
- Kopycki, J.G., Stubbs, M.T., Brandt, W., Hagemann, M., Porzel, A., Schmidt, J., Schliemann, W., Zenk, M.H., Vogt, T., 2008. Functional and structural characterization of a cation-dependent O-methyltransferase from the cyanobacterium *Synechocystis* sp. strain PCC 6803. *J. Biol. Chem.* 283, 20888–20896.
- Lee, Y.J., Kim, B.G., Chong, Y., Lim, Y., Ahn, J.-H., 2008. Cation dependent O-methyltransferases from rice. *Planta* 227, 641–647.
- Lucker, J., Martens, S., Lund, S.T., 2010. Characterization of a *Vitis vinifera* cv. Cabernet Sauvignon 3',5'-O-methyltransferase showing strong preference for anthocyanins and glycosylated flavonols. *Phytochemistry* 71, 1474–1484.
- Lukacin, R., Matern, U., Specker, S., Vogt, T., 2004. Cations modulate the substrate specificity of bifunctional class I O-methyltransferase from *Ammi majus*. *FEBS Lett.* 577, 367–370.
- Noel, J.P., Dixon, R.A., Pichersky, E., Zubieta, C., Ferrer, J.L., 2003. Structural, functional, and evolutionary basis for methylation of plant small molecules. *Recent Adv. Phytochem.* 37, 37–58.
- Schmittgen, T.D., Livak, K.J., 2008. Analyzing real-time PCR data by the comparative C-T method. *Nat. Protoc.* 3, 1101–1108.
- Tamura, K., Peterson, D., Peterson, N., Stecher, G., Nei, M., Kumar, S., 2011. MEGA5: molecular evolutionary genetics analysis using maximum likelihood, evolutionary distance, and maximum parsimony methods. *Mol. Biol. Evol.* 28, 2731–2739.
- Vogt, T., 2004. Regiospecificity and kinetic properties of a plant natural product O-methyltransferase are determined by its N-terminal domain. *FEBS Lett.* 561, 159–162.
- Weng, J.-K., Chapple, C., 2010. The origin and evolution of lignin biosynthesis. *New Phytol.* 187, 273–285.
- Widiez, T., Hartman, T.G., Dudai, N., Yan, Q., Lawton, M., Havkin-Frenkel, D., Belanger, F.C., 2011. Functional characterization of two new members of the caffeoyl CoA O-methyltransferase-like gene family from *Vanilla planifolia* reveals a new class of plastid-localized O-methyltransferases. *Plant Mol. Biol.* 76, 475–488.
- Willits, M.G., Giovanni, M., Prata, R.T.N., Kramer, C.M., De Luca, V., Steffens, J.C., Graser, G., 2004. Bio-fermentation of modified flavonoids: an example of in vivo diversification of secondary metabolites. *Phytochemistry* 65, 31–41.
- Zhou, J.-M., Gold, N.D., Martin, V.J.J., Wollenweber, E., Ibrahim, R.K., 2006. Sequential O-methylation of tricetin by a single gene product in wheat. *Biochim. Biophys. Acta* 1760, 1115–1124.